Krugh, T. R., and Reinhardt, C. G. (1975), *J. Mol. Biol. 97,* 133-162.
Ladner, J. E., Jack, A., Robertus, J. D., Brown, R. S., Rhodes, D., Clark, B. F. C., and Klug, A. (1975), *Nucleic Acids Res. 2,* 1629-1637.
LePecq, J. B., and Paoletti, C. (1967), *J. Mol. Biol. 27,* 87.
Liebman, M., Rubin, J., and Sundaralingam, M. (1977), *Proc. Natl. Acad. Sci. U.S.A. 74,* 4821-4825.
Loeb, L. A. (1974), *Enzymes, 3rd Ed. 10,* 173-209.
Lurquin, P., and Buchet-Mahieu, J. (1971), *FEBS Lett. 12,* 244-248.
Olmsted, J., and Kearns, D. R. (1977), *Biochemistry 16,* 3647-3654.
Patel, D. J., and Canuel, L. L. (1976), *Proc. Natl. Acad. Sci. U.S.A. 73,* 3343-3347.
Quigley, G. J., Seeman, N. C., Wang, A. H. J., Suddath, F. L., and Rich, A. (1975), *Nucleic Acids Res. 2,* 2329-2341.
Reid, B. R., Ribeiro, N. S., Gould, G., Robillard, G., Hilbers, C. W., and Shulman, R. G. (1975), *Proc. Natl. Acad. Sci. U.S.A. 72,* 2049-2053.
Robillard, G. T., and Kim, S. H. (1976), in Abstracts, VIII International Conference on Magnetic Resonance in Biological Systems.
Robillard, G. T., Tarr, C. E., Vosman, F., and Berendsen, H. J. C. (1976a), *Nature (London) 262,* 363-369.
Robillard, G. T., Hilbers, C. W., Reid, B. R., Gangloff, J., Dirheimer, G., and Shulman, R. G. (1976b), *Biochemistry 15,* 1883-1888.
Sakai, T. T., Torget, R. I. J., Freda, C. E., and Cohen, S. S. (1975), *Nucleic Acids Res. 2,* 1005-1021.
Shulman, R. G., Hilbers, C. W., Kearns, D. R., Reid, B. R., and Wong, Y. P. (1973), *J. Mol. Biol. 78,* 57-69.
Stout, C. D., and Sundaralingam, M. (1975) Abstract, Regional Meeting of the American Chemical Society,
Stout, C. D., Mizuno, H., Rubin, J., Brennan, T., Rao, S. T., and Sundaralingam, M. (1976), *Nucleic Acids Res. 3,* 1111-1123.
Sussman, J. L., and Kim, S. H. (1976), *Biochem. Biophys. Res. Commun. 68,* 89-96.
Surovaya, A. N., and Borissova, O. F. (1976), *Mol. Biol. Rep. 2,* 487-495.
Tritton, T. R., and Mohr, S. C. (1973), *Biochemistry 12,* 905-914.
Tsai, C. C., Jain, S. C., and Sobell, H. M. (1975), *Proc. Natl. Acad. Sci. U.S.A. 72,* 628-632.
Urbanke, C., Romer, R., and Maass, G. (1973), *Eur. J. Biochem. 33,* 511-516.
Waring, M. J. (1965), *J. Mol. Biol. 13,* 269-282.
Waring, M. J. (1974), *Biochem. J. 143,* 483-486.
Waring, M. J. (1975), in Antibiotics III, Corcoran, J. W., and Hahn, F. E., Ed., New York, N.Y., Springer-Verlag, pp 141-165.
Warrant, R. W., Sussman, J. L., and Kim, S. H. (1976), Abstracts, 67th Meeting of the American Society of Biological Chemistry, paper no. 1922.
Wells, B. D., and Cantor, C. R. (1977), *Nucleic Acids Res. 4,* 1667-1680.
Wong, K. L., and Kearns, D. R. (1974), *Nature (London) 252,* 738-739.
Wong, K. L., Bolton, P. H., and Kearns, D. R. (1975), *Biochim. Biophys. Acta 383,* 446-451.

# Physical Characterization of Myosin Light Chains†

Walter F. Stafford III* and Andrew G. Szent-Györgyi

ABSTRACT: This paper reports the results of an investigation into the size and shape of the low molecular weight subunits (light chains) of myosin from several animal species. Hydrodynamic, analytical gel filtration, and fluorescence anisotropy decay measurements indicated that these light chains could be represented by a general ellipsoidal model having a longest axis of about 100 ± 20 Å. Investigation into the stability of the internal structure of the scallop regulatory light chain was carried out by studying the effect of pH, ionic strength, temperature, and guanidine hydrochloride on its circular dichroic spectrum. The nearly complete insensitivity of the circular dichroic spectrum to pH, ionic strength, and temperature variations from 4 to 70 °C indicated that this subunit contained regions of very stable structure which probably exist when it is bound to myosin.

The myosin molecule is a hexameric enzyme comprised of two large polypeptide chains of about 200 000 and two pairs of low molecular weight polypeptide chains ranging from 17 000 to 25 000. The low molecular weight subunits can be divided into two classes on the basis of their chemical structure, electrophoretic mobilities, and the methods used to dissociate them from myosin.

Light chains of one class can be removed only with concomitant loss of ATPase activity and have been called alkali-light chains in rabbit (Gazith et al., 1970; Weeds, 1969) and SH-light chains in the myosin regulated adductor muscle of scallop (Szent-Györgyi et al., 1973). On the basis of the loss of ATPase activity with removal of light chains by various agents, a direct role of the myosin light chains in the ATPase activity and ADP binding of myosin was postulated by Gershman et al. (1968, 1969), Dreizen et al. (1967), Dreizen and Gershman (1970), and Dreizen and Richards (1973). More recently, it has been demonstrated that the two different types of alkali-light chains (alkali-1 and alkali-2) have no effect

† From the Department of Biology, Brandeis University, Waltham, Massachusetts 02154. *Received August 4, 1977.* This research was generously supported by a grant from the Public Health Service (AM 15963 to A.G.S.G.) and a Fellowship from the Muscular Dystrophy Association of America (to W.F.S.).

0006-2960/78/0417-0607$01.00/0 

on the potassium and calcium ATPase activities but do modulate the actin activated Mg-ATPase activity of rabbit myosin (Wagner and Weeds, 1977). There are also indications that the different types of alkali-light chains may affect the affinity of S-1[1] for actin even in the absence of ATP (Winstanley et al., 1977). Light chains of the second class can be removed without loss of ATPase activity and have been called the DTNB light chains in rabbit and the EDTA or regulatory light chains in molluscan and other muscles exhibiting myosin-linked regulation.

Myosin-linked regulation and a combination of both actin and myosin-linked regulation are widely distributed throughout the animal kingdom (Lehman and Szent-Györgyi, 1975). Many details of the mechanism of actin-linked regulation are known at the molecular level. Much less, however, is known about the molecular details of myosin-linked regulation or the interrelationships of the myosin subunits in the mechanism of the regulatory process (Szent-Györgyi, 1976). Knowledge of the size and shape of the myosin light chain subunits is fundamental to a full understanding of both their role in controlling myosin ATPase, in general, and the mechanism of myosin-linked regulatory systems, in particular.

Tsao (1953) was the first to attempt a physical characterization of myosin subunits. On a mixture of subunits obtained by fast urea dissociation, he measured an average molecular weight of 16 000 and an axial ratio of around 12 using osmotic pressure, viscosity, and fluorescence polarization techniques. The average molecular weight and frictional ratio of the alkali dissociable low molecular weight fraction of myosin were also determined by Gershamn et al. (1966), who found an average molecular weight of 20 200 and a frictional ratio of 1.41. However, Holt and Lowey (1975a,b) were the first to perform a physical characterization of purified rabbit DTNB light chains and found a molecular weight of 19 300. Their CD data indicated the presence of a considerable amount of $\alpha$-helical structure.

The investigation reported here was carried out to obtain information about the structure of these subunits. The DTNB light chain of rabbit skeletal muscle myosin, regulatory light chains from four molluscan species, and the SH-light chain from scallop were examined to determine their overall structure and conformation in solution. This investigation forms part of a larger inquiry into the interactions between light chains and myosin heads during the regulatory process and their precise role in the mechanism of regulation. Some of the work described in this communication has been presented previously (Stafford and Szent-Györgyi, 1976).

## Materials and Methods

*Isolation and Purification of Light Chains.* Isolation and purification of the light chains were carried out as described earlier (Szent-Györgyi et al., 1973; Kendrick-Jones et al., 1976). Light chains were obtained from *Spisula solidissima* (surf clam), *Mercenaria mercenaria* (hard shell clam), *Aequipecten irradians* (bay scallop), *Loligo pealei* (squid), and *Oryctologus cuniculus* (rabbit).

*Sedimentation and Diffusion Analysis.* Sedimentation coefficients and molecular weights were measured with a Spinco Model E analytical ultracentrifuge using the Rayleigh interference or Schlieren optical systems. Capillary-type synthetic boundary cells (12 and 30 mm) were used for measuring the sedimentation coefficient of the scallop regulatory light chain. The sedimentation coefficients were calculated from the movement of the boundary at half-plateau concentration with the Rayleigh optical system or movement of maximum of the gradient curve with the Schlieren system. Most determinations were done at 44 000 rpm in an An-E rotor. The solvent was 0.5 M NaCl, 0.01 M phosphate, 0.0015 M $CaCl_2$, 0.0015 $MgCl_2$, 0.001 M EDTA, pH 7.5. $MgCl_2$ was included since it is part of the normal in vivo ionic milieu. $CaCl_2$ was included since initially we had the expectation that $CaCl_2$ might mediate a dimerization of the light chain. EDTA was included to sequester heavy metal ions. In 0.5 M NaCl the nonideality from the Donnan effect in equilibrium centrifugation and diffusion and the primary charge effect in velocity sedimentation (Pedersen, 1958) are reduced, so that they would not be expected to make a significant contribution under these conditions. It was calculated, according to the method of Roark and Yphantis (1971), that the Donnan equilibrium would result in a maximum expected reduction in the apparent molecular weight of the scallop regulatory light chain at 1 mg/mL of 1.5% in 0.5 M NaCl since it carries a maximum charge of about $z = -12$ at pH 7.5. In general, the observed effects from the Donnan equilibrium are less than those calculated because of counter ion binding (Szuchet and Yphantis, 1973). Diffusion measurements were made using capillary type synthetic boundary cells both at low speed (6000 rpm) and during sedimentation velocity runs (44 000 rpm). All solutions were dialyzed for at least 48 h and handled quickly in the cold room while loading the cells to minimize evaporation. Relative humidity in the cold room was 70–75%. When the Rayleigh optical system was used, diffusion coefficients were estimated by measuring the standard deviation of the integral ($C$ vs. $r$) boundary in the following manner: For a given concentration span, $\Delta C$, centered at the midpoint of the boundary, one can estimate the diffusion coefficient from the following equation:

$$Dt = \left( \frac{\Delta r}{4\mathrm{erf}^{-1}\mathrm{0base}\left(\frac{\Delta C}{C_p}\right)} \right)^2 \qquad (1)$$

where $D$ is the diffusion coefficient, $t$ is the time from the formation of the boundary, $\Delta r$ is the span in the radial direction corresponding to the concentration span $\Delta C$, $C_p$ is the plateau concentration, $\mathrm{erf}^{-1}$ is the inverse error function, and erf is the error function which is defined in terms of the probability integral by

$$\mathrm{erf}(x) = \frac{2}{\sqrt{\pi}} \int_0^x e^{-x^2} \mathrm{d}x \qquad (2)$$

where $x$ is displacement from the center of the boundary in units of $\sqrt{4Dt}$. Several concentration spans were used, and $D$ was obtained by plotting values of $Dt$ against time and taking the slope. Values of the error function were calculated using a rational approximation given by Gautschi (1965). Use of the error function to describe the shape of the diffusing boundary was justified since the material was homogeneous, showed no concentration dependence, and therefore was expected to exhibit a Gaussian boundary.

Equation 1 was derived from the definition of the error function and several relations given by Tanford (1961). This method of determining diffusion coefficients is similar to a method described by Svedberg and Pedersen (1940) and to one described by Haschemeyer and Haschemeyer (1973). Alternatively, when diffusion coefficients were measured from

[1] Abbreviations used: ATP, adenosine triphosphate; ADP, adenosine diphosphate; S-1, myosin subfragment 1; DTNB, 5,5′-dithiobis(2-nitrobenzoic acid); EDTA, ethylenediaminetetraacetic acid; Gdn·HCl, guanidine hydrochloride.

Schlieren photographs, the square of the peak width at half-height was plotted against time. It can be readily shown that the slope of this plot is given by $16D$ ln 2. Values of $D$ were averaged since no significant concentration dependence was observed. Although the precision attainable by either method within a given run was about 2–3%, the possible sources of systematic error associated with the use of synthetic boundary cells contributed somewhat greater uncertainty to the measurements.

The systematic errors arise from the use of synthetic boundary cells primarily when concentrated salt solutions (0.5 M NaCl) are used. A relatively small mismatch in salt concentration between the sample and the buffer solutions can lead to gross errors in the measurement of $s$ and $D$. For example, a mismatch of $5 \times 10^{-3}$ M (1% error) in NaCl concentration would be expected to result in an error of about one fringe in total concentration in a 12-mm cell (one fringe in a 12-mm cell corresponds to about 0.25 mg/mL of protein); therefore, even a small mismatch would result in the superposition of an appreciable NaCl boundary on the protein boundary if protein concentrations were only 1–2 mg/mL as used in this study. The values of $s$ and $D$ obtained would then be average values for the protein and NaCl. Since the boundary moves only about 400 $\mu$m during the run, the presence of the salt would cause skewing of the boundary which would be manifested in unusually high diffusion coefficients and low sedimentation coefficients. Convection in the boundary at these low protein concentrations is another possible source of error. A value of $D$ was measured for each sedimentation velocity run, and ratios of $s/D$ were compared with the known molecular weight through the Svedberg equation. Thus, runs that did not give values of $s$ and $D$ consistent with the known molecular weight were discarded.

The Stokes' radius, $R_s$, obtained from sedimentation and diffusion was calculated from the following relationships:

$$R_{s,sed} = M_2(1 - \bar{v}_2\rho)/6N\pi\eta_0 s^0_{20,w} \quad (3)$$

$$R_{s,diff} = kT/6\pi\eta_0 D^0_{20,w} \quad (4)$$

where $R_s$ is the Stokes' radius, $M_2$ is the molecular weight, $\bar{v}_2$ is the partial specific volume of the protein, $\rho$ is the density of the solution, $N$ is Avogadro's number, $\eta_0$ is the solvent viscosity, $s^0_{20,w}$ is the intrinsic sedimentation coefficient at infinite dilution, $k$ is Boltzman's constant, $T$ is the absolute temperature (K), $D^0_{20,w}$ is the infinite dilution value of the diffusion coefficient referred to water at 20 °C. Partial specific volumes were calculated from the amino acid composition (Cohn and Edsall, 1941).

*Fluorescence Decay Anisotropy Measurements.* Measurements of fluorescence decay anisotropy were carried out for us by Drs. S. C. Harvey and H. C. Cheung. Fluorescence lifetime and decay anisotropy curves were measured with a single photon fluorometer (Yguerabide, 1972). The decay curves were deconvoluted with a computer program based on the method of moments (Isenberg et al., 1973). Details of the equipment and procedures are described elsewhere (Harvey and Cheung, 1977).

*Molecular Weight Determinations.* Molecular weight determinations were made using the high speed equilibrium method of Yphantis (1964) and the improved cell components and techniques of Ansevin et al. (1970). The collimating lens of the optical system was equipped with a specially constructed externally adjustable, motor-driven interference slit assembly, capable of rotational adjustment to within ±0.01° (Stafford, submitted for publication). Point by point molecular weight averages were calculated using the computer program of Roark and Yphantis (1969). Each protein solution was dialyzed exhaustively against its buffer (Cassasa and Eisenberg, 1964).

*Analytical Gel Filtration: Determinationof Stokes' Radius.* Analytical gel filtration measurements were made with a 0.9 × 100 cm column packed with Sephadex G-150 (lot no. 9850). The column was calibrated according to the method of Ackers (1967) with ribonuclease, ovalbumin, bovine serum albumin, and aldolase. Separate standard curves were made at high and low ionic strength. The value of the Stokes' radius of each of the standard proteins was calculated from the equation of Stokes and Einstein (eq 4) and values of diffusion coefficients given in Table XV of the article by Kuntz and Kauzman (1974). The value of the Stokes' radius, $R_s$, of the various light chains was estimated from the following relationship (Ackers, 1967):

$$R_s = a_0 + b_0 \mathrm{erfc}^{-1}(\sigma)$$

where $\mathrm{erfc}^{-1}(\sigma)$ is the inverse compliment error function defined below, $a_0$ and $b_0$ are the column calibration constants obtained by plotting $R_s$ for the known proteins versus $\mathrm{erfc}^{-1}(\sigma)$ where $\sigma$ is the partition coefficient defined by

$$\sigma \equiv (V_e - V_0)/(V_x - V_0)$$

where $V_e$, $V_0$, and $V_x$ are the elution volumes of the protein, totally excluded material, and totally included material, respectively. The inverse compliment error function is related to the error function in the following way: If $y = \mathrm{erfc}(x) = 1 - \mathrm{erf}(x)$, then $\mathrm{erfc}^{-1}(y) = x$, where $\mathrm{erf}(x)$ is defined above by eq 2. The use of the error function to linearize the relationship between Stokes' radius and the partition coefficient relies on the assumption that the pore size distribution within the gel can be described by a Gaussian distribution. Validity of this assumption appears to be borne out by experiment (Ackers, 1967, 1970).

The advantages of using analytical gel filtration instead of sedimentation and diffusion measurements were twofold: First, the salt mismatch problems mentioned above associated with handling samples for synthetic boundary runs did not effect the results of gel filtration; and second, the column was long enough to resolve monomers from dimers and aggregates of these light chains obtained from species other than scallop. Some dimers and aggregates were occasionally present in samples of those light chains which contained sulfhydryl groups.

*Circular Dichroism Measurements.* Circular dichroic (CD) spectra were measured with a Cary 60 recording spectropolarimeter with a Model 6001 CD attachment equipped with a programmed slit control to give a 1.5-nm bandwidth. Spectra were determined in 0.01 M phosphate, pH 7.5, and 0.1 M or 0.5 M NaF, 0.01 M phosphate, pH 7.5, to obtain measurements down to 185 nm. Control spectra were also measured in 0.1 M NaCl to show that NaF did not denature the light chains. Spectra in NaCl could be measured only as far down as 210 nm so that changes in structure manifested between 210 and 185 nm could not be ruled out. However, it seems reasonable to assume that lack of changes in the region between 260 and 210 nm probably indicates lack of significant changes in the region between 210 and 185 nm since the $\alpha$ helical and $\beta$ structures would be expected to contribute to both regions of the spectrum. The concentrations of the light chains were estimated spectrophotometrically. The following extinction coefficients, $E^{1\%}_{280nm,1cm}$, were used: scallop (regulatory), 2.0; scallop (-SH), 5.5; *Mercenaria,* 5.0; *Spisula,* 4.6; *Loligo,* 4.6. The CD spectra were analyzed according to the least-squares procedure of Greenfield and Fasman (1969), using their basis

TABLE I: Summary of Physical Properties Determined for the Scallop Myosin Regulatory Subunit by Ultracentrifugal Analysis.[a]

| | |
|---|---|
| $s^0_{20,w}$ | = 1.69 ± 0.1 S |
| $D_{20,w}$ | = 8.30 ± 0.5 F |
| $M_{s/D}$ | = 17 700 ± 1000 amu |
| $M_{Eq}$ | = 18 100 ± 500 amu |
| $R_0$ | = 17.4 Å |
| $R_{S,sed}$ | = 26.5 ± 1.3 Å |
| $R_{S,diff}$ | = 26.2 ± 1.5 Å |
| $f/f_{min}$ | = 1.52 |
| $\bar{v}_2$ | = 0.721 $cm^3/g$[b] |
| $\delta_1$ | = 0.45 $g/g$[b] |

[a] The diffusion coefficient is the average value from two determinations for which it was fairly certain that evaporation or convection was not a problem. The error bar is the root mean square (rms) of the standard error of estimate for each determination. The sedimentation coefficient at zero concentration was obtained from four protein concentrations. [b] Calculated from amino acid composition.

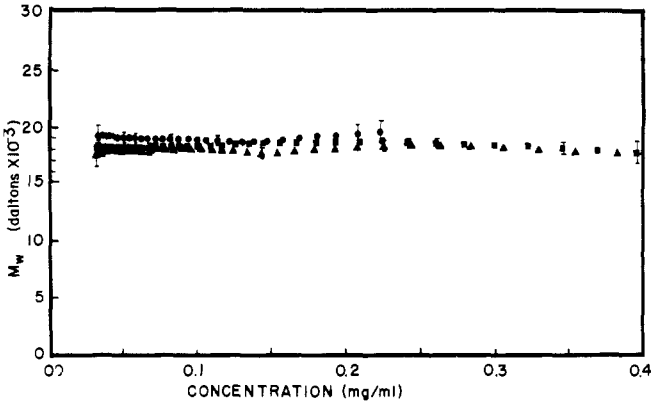


FIGURE 1: High-speed equilibrium ultracentrifugation of the scallop regulatory light chain in 0.5 M NaCl, 0.010 M phosphate, 0.0015 M $MgCl_2$, 0.0015 M $CaCl_2$, 0.0010 M EDTA, pH 7.5, at three loading concentrations: (●) 0.08 mg/mL; (■) 0.27 mg/mL; and (▲) 0.80 mg/mL. ($\omega$) = 44 000 rpm; $T$ = 276 K; 30 mm, Yphantis six-channel center piece.

TABLE II: Stokes' Radii of Myosin Light Chains Determined by Analytical Gel Filtration on Sephadex G-150.

| | $R_s$ (Å) | |
|---|---|---|
| Regulatory light chains | In 0.5 M NaCl | In 0.01 M phosphate |
| Scallop | 25.5 | 26.7 |
| *Mercenaria* | 25.9 | 25.7 |
| *Spisula* | 26.7 | 24.6 |
| *Loligo* | 25.5 | 25.4 |
| Rabbit | 25.9 | |
| Scallop SH-light chain | | 27.3 |

spectra as reference spectra for $\alpha$ helix, $\beta$ sheet, and polylysine random structure. Least-squares fits were done also using the spectrum of the scallop regulatory light chain in 6 M Gdn·HCl as a random basis spectrum between 210 and 260 nm.

## Results and Interpretations

*Sedimentation Equilibrium: Molecular Weight and Determination of Homogeneity.* The molecular weight of the scallop regulatory light chain found by the high-speed equilibrium method was 18 100 ± 500 amu, using a value of 0.725 $cm^3/g$ for the partial specific volume calculated from the amino acid composition and corrected to pH 7.5 using the Scatchard definitions of components (Tanford, 1961) (Table I). The plots of weight average molecular weight ($M_w$) vs. concentration for three different loading concentrations (Figure 1) overlap within experimental error indicating that the light chain preparations are thermodynamically homogeneous (Squire and Li, 1961; Yphantis, 1964). A value of 17 400 ± 1000 amu was found by combining the results of sedimentation and diffusion. These values compare well with the molecular weight of 17 229 for the isoelectric light chain calculated from the amino acid sequence (Kendrick-Jones and Jakes, 1977). If the partial specific volume used to calculate the molecular weight of the light chain had been measured in this solvent and the molecular weight corrected for component definition and preferential interactions, perhaps better agreement would have been obtained (Casassa and Eisenberg, 1964).

*Stokes' Radius Determination.* The Stokes' radius of the scallop regulatory light chain obtained from sedimentation velocity experiments was calculated from eq 3 using the value of $M_2(1 - v_2\rho)$ obtained from the sedimentation equilibrium experiments, while the value obtained from diffusion measurements was calculated directly by substituting $D$ into eq 4. Values observed (Table I) were 26.5 ± 1.3 and 26.2 ± 1.5 Å from sedimentation and diffusion, respectively.

From the results of analytical gel filtration (Table II), the four molluscan regulatory light chains and the rabbit DTNB light chains appeared to be the same size within experimental error with an average value of $R_s$ of 25.9 ± 0.5 Å. The scallop SH-light chain may be slightly larger with a measured Stokes' radius of 27.3 Å; however, the difference is not statistically significant. Since all these light chains have very nearly the same molecular weight, they have a maximum frictional ratio of about 1.5 and would seem to be similarly asymmetric.

*Light Chain Geometry.* The maximum frictional ratio, $(f/f_{min})$, was calculated from $(f/f_{min}) = R_s/R_0$, where $f$ is the frictional coefficient for the light chain, $f_{min}$ is the frictional coefficient for the equivalent unhydrated sphere, $R_s$ is the Stokes radius of the light chain, and $R_0$ is the Stokes radius of the equivalent unhydrated sphere. The radius of the equivalent unhydrated sphere was calculated from eq 5 and was estimated to be 17.4 Å. Any error in $(f/f_{min})$ resulting from use of the calculated value of the partial specific volume will not significantly alter the conclusions about the asymmetry of the light chains since errors arise only through $R_0$ from the product $M_2\bar{v}_2$ (see eq 5).

$$R_0 = (3M_2\bar{v}_2/4\pi N)^{1/3} \quad (5)$$

The percent error in the product $M_2\bar{v}_2$ is about four times the percent error in $\bar{v}_2$ so that the percent error in $R_0$ and $(f/f_{min})$ will be only about 1.3 times the percent error in $\bar{v}_2$.

It should be noted that, for values of $(f/f_{min})$ in the range observed for the light chains, measurements of the frictional coefficient alone cannot distinguish an asymmetric particle from a swollen sphere or random coil, and, therefore, independent measurements were carried out to decide this question. The possibility that the light chain existed as a "denatured" swollen particle in solution was investigated both by studying the circular dichroism spectra to determine the amount and stability of ordered structure and by studying the fluorescence decay anisotropy. Anisotropy decay measurements can distinguish unequivocally between an asymmetric and a spherically symmetric particle in solution for models other than an

TABLE III: Dimensions of Unhydrated General Ellipsoidal Models for Myosin Light Chains.

| $(f/f_{min})$ = 1.5 | | $r_1 = a/b$; $r_2 = b/c$ | | |
|---|---|---|---|---|
| $r_1$ | $r_2$ | $2a$ | $2b$ | $2c$ |
| | | $\delta_1 = 0.45$; $f/f_0 = 1.28$ | | |
| 5.5 | 1.0 | 108 | 19.7 | 19.7 |
| 3.6 | 2.0 | 103 | 28.6 | 14.3 |
| 2.5 | 3.0 | 92 | 36.8 | 12.3 |
| 1.8 | 4.0 | 82 | 45.4 | 11.4 |
| | | $\delta_1 = 0.35$; $f/f_0 = 1.32$ | | |
| 6.1 | 1.0 | 116 | 19.0 | 19.0 |
| 4.0 | 2.0 | 110 | 27.6 | 13.8 |
| 2.8 | 3.0 | 100 | 35.6 | 11.9 |
| 2.2 | 4.0 | 93 | 42.5 | 10.6 |
| | | $\delta_1 = 0.19$; $f/f_0 = 1.39$ | | |
| 7.2 | 1.0 | 130 | 18.0 | 18.0 |
| 4.8 | 2.0 | 125 | 26.0 | 13.0 |
| 3.5 | 3.0 | 116 | 33.0 | 11.0 |
| 2.7 | 4.0 | 107 | 39.6 | 9.9 |
| | | $a = R_0(r_1^2 r_2)^{1/3}$ | | |

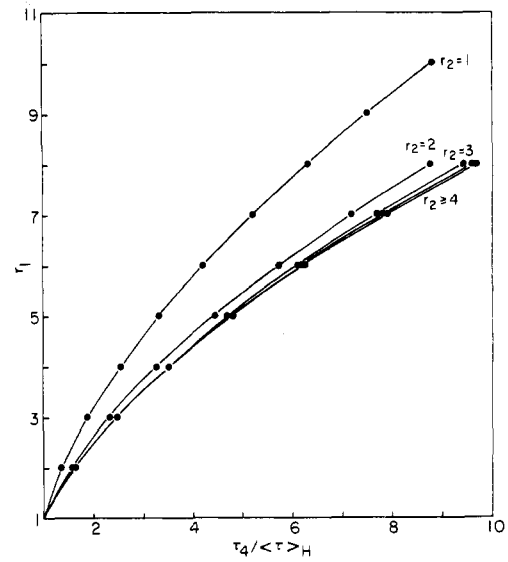


FIGURE 2: Values of the axial ratios for the general ellipsoidal model as a function of the ratio, $\tau_4/\langle\tau\rangle_H$, as defined in the text. (Computed from the calculations of Small and Isenberg (1977).) This ratio can be used to set limits for $r_1$.

oblate ellipsoid of revolution.

*Fluorescence Decay Anisotropy Measurements.* The fluorescence decay anisotropy of the scallop and *Mercenaria* regulatory light chains showed two component decay curves with decay times of 15 and about 80 ns with amplitudes of 0.16 and 0.08 for scallop and 12 and about 70 ns with amplitudes of 0.15 and 0.06 for *Mercenaria,* respectively. The presence of two decay times rules out a swollen sphere or random coil model. The data fit a prolate ellipsoidal model with a maximum frictional ratio of about 1.5 which agrees very well with the hydrodynamic data. A more detailed analysis of this data in combination with the hydrodynamic data is given below.

*Ellipsoidal Models.* Various ellipsoidal models for the light chains were considered using the numerical solutions of Small and Isenberg (1977) for the equations of Perrin for the general ellipsoid. In the use of the general Perrin equations two axial ratios are specified. The ratio of the largest axis to the intermediate axis is designated $r_1$ and that of the intermediate axis to the smallest axis is designated $r_2$. The two extreme cases for which analytical solutions to these equations were obtained by Perrin are for $r_1 = 1$ (the oblate ellipsoid) and for $r_2 = 1$ (the prolate ellipsoid). The general solutions to the Perrin equations allow consideration of intermediate values of $r_1$ and $r_2$. In general, for any given value of $f/f_0$ there will be an infinite number of possible paired values of $r_1$ and $r_2$, ranging from the purely prolate to the purely oblate ellipsoidal model (see their Figure 2). Table III gives the dimensions of various unhydrated ellipsoidal models that are consistent with the observed maximum frictional ratio obtained from hydrodynamic and analytical gel filtration measurements. A value of the maximum hydration of 0.45 g/g was calculated from the amino acid composition by the method of Kuntz and Kauzmann (1974) without making any corrections for residues inaccessible to the solvent. Other values of assumed hydration are presented to show the range of possible shapes. It can be shown that the longest semi-axis, $a$, for the general ellipsoid is given by

$$a = R_0(r_1^2 r_2)^{1/3} \quad (6)$$

where $R_0$ is the radius of the equivalent sphere, and $r_1$ and $r_2$ are the axial ratios obtained for a specified value of $f/f_0$, where $f/f_0$ is the contribution to the maximum frictional ratio from shape alone. The maximum frictional ratio $(f/f_{min})$ and $f/f_0$ are related by

$$f/f_0 = (f/f_{min})(v_2/(v_2 + \delta_1 v_1^\circ))^{1/3}$$

where $\delta_1$ is the degree of hydration expressed as grams of water bound per gram of protein and $v_1^\circ$ is the partial specific volume of pure water (Tanford, 1961).

The values given in Table III were chosen for three degrees of hydration and represent possible ellipsoidal models ranging from purely prolate to progressively more nearly oblate. As one can see for each assumed degree of hydration, as $r_1$ approaches 1.0, the model becomes successively flattened. The case for $r_2$ equal to 4 seems to have approached an unrealistically small thickness; therefore, models more nearly approaching the oblate ellipsoid are considered to be untenable. The oblate model is ruled out completely by the fluorescence anisotropy data since a single exponential decay is expected for an oblate ellipsoid.

By combining the hydrodynamic and fluorescence anisotropy decay data, one can determine both the degree of hydration and the axial ratios of rigid ellipsoidal models, in principle, if the three expected anisotropy lifetimes for such a particle can be resolved. In practice, only two of the lifetimes have ever been resolved, and therefore one can obtain only limits to the hydration and range of possible ellipsoidal shapes. By plotting values of $r_1$ vs. $r_2$ for values of both $f/f_0$ and the anisotropy lifetimes, following the general procedure of Small and Isenberg (1977), one can set rather stringent limits to these parameters. First, however, we define a new function of the anisotropy lifetimes which is independent of any assumptions of the hydration. By inspection of the Table I of Small and Isenberg, one can see that the theory predicts five anisotropy decay times, $\tau_i$, associated with each ellipsoidal model. These are grouped into two pairs of nearly equal short times, $\tau_1$, $\tau_2$, $\tau_3$, and $\tau_5$ and a single longer time, $\tau_4$. Experimentally, the observed short decay time will be nearly equal to the harmonic mean $(\langle\tau\rangle_H)$ of $\tau_1$, $\tau_2$, $\tau_3$, and $\tau_5$ while the longer decay time will be equal to $\tau_4$. The ratio of $\tau_4$ to $\langle\tau\rangle_H$ is an experimentally observable quantity which is independent of any assumptions about hydration. Values of $r_2$ and $r_1$ for this ratio can be cal-

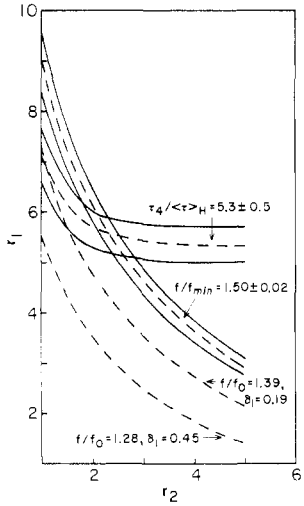


FIGURE 3: Values of $r_1$ and $r_2$ consistent with the observed hydrodynamic and fluorescence anisotropy decay data. Plotted from observed values of $\tau_4/\langle\tau\rangle_H$ and $f/f_{min}$.

culated from the tabulated solutions of Small and Isenberg (see Figure 2) and plotted to obtain possible ellipsoidal models consistent with the anisotropy data. It is interesting to note that $r_1$ is relatively insensitive to changes in $r_2$ for $r_2 \geq 2$ and, therefore, can be used to set a lower limit on $r_1$ for a particular value of $\tau_4/\langle\tau\rangle_H$. If the hydration is known independently, the plot of $r_1$ vs. $r_2$ for $f/f_0$ will intersect the plot of $r_1$ vs. $r_2$ for $\tau_4/\langle\tau\rangle_H$ at a point which uniquely determines the axial ratios of the ellipsoidal model. If the hydration is unknown, one can obtain limits for the axial ratios and the hydration. The curves for $r_1$ vs. $r_2$ for $(f/f_{min})$ and two values of $f/f_0$ (for $\delta_1 = 0.19$ and 0.45) and for $\tau_4/\langle\tau\rangle_H$ are plotted in Figure 3. Clearly, the case for $\delta_1 = 0.45$ is inconsistent with the fluorescence anisotropy data, while the case for $\delta_1 = 0.19$ gives an upper limit to the hydration. At the same time, the limiting curve for $(f/f_{min})$ indicated that ellipsoidal models with $r_2$ greater than about 2.5 and $r_1$ less than about 5.3 do not represent the data. The prolate ellipsoid of revolution ($r_2 = 1$) seems to give the best fit to the data since the hydration probably is not much less than 0.20. Although the success of this type of analysis depends on the rather naive assumption that the light chains can be represented by rigid ellipsoids, one can conclude probably quite safely that the light chains are asymmetric and seem to have a length of about 100 ± 20 Å, not including hydration.

*Internal Structure and Stability.* The existence of appreciable amounts of ordered structure in the scallop regulatory light chain in solution is indicated from a comparison of the far and near ultraviolet (UV) CD spectra in phosphate and in 6 M Gdn·HCl (Figures 4a and 4b). The CD spectrum of the light chain was temperature independent from 40 to 70 °C indicating that the internal structure of the light chain which gives rise to the CD spectrum is very stable. The changes in the tyrosine and phenylalanine regions in Gdn·HCl demonstrate a contribution to the spectrum from the tertiary organization of the polypeptide chain (Sears and Beychok, 1973). This observation is important in connection with the problem of whether or not the light chain has become denatured upon detachment from the myosin head. Although limited unfolding may have occurred upon removal of the regulatory light chain from myosin, the stability of the remaining structure in solution is an indication that probably there have not been large alterations in the structure. One might argue that the loss of calcium binding indicates partial unfolding, but it has not been shown yet whether or not the heavy chain also is involved in calcium

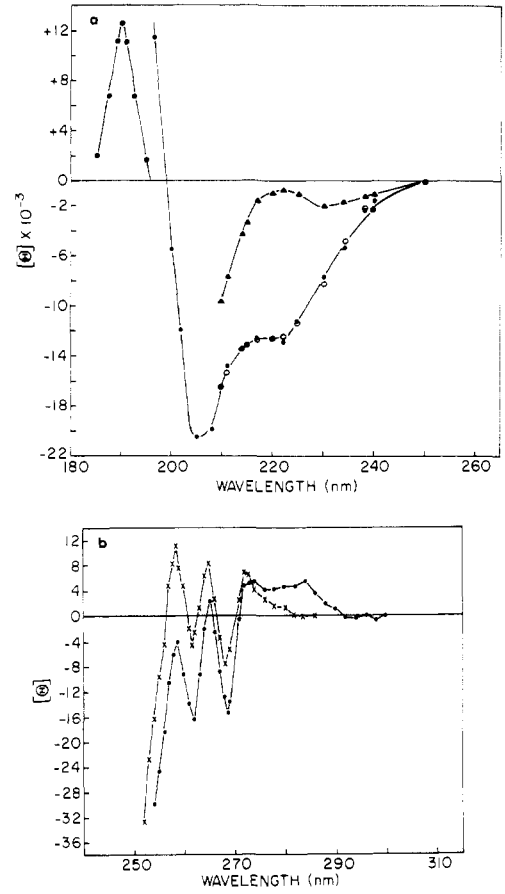


FIGURE 4: (a and b) Circular dichroism spectra of the scallop regulatory light chain (●) in 0.01 M phosphate, pH 7.5, and (▲, X) 6 M Gdn·HCl, 0.01 M phosphate, pH 7.5; (○) least-squares fit using light chain random basis spectrum in 6 M Gdn·HCl as explained in text.

binding (Kendrick-Jones et al., 1976). The tertiary organization of the scallop regulatory light chain in solution appears to be highly specific since it can be renatured readily from both concentrated urea and Gdn·HCl solutions to yield a molecule functionally active in regulation.

The far UV CD spectrum at pH 7.5 was found to be invariant with ionic strength over a range from 0.02 to 0.5 and no significant variation was found with calcium ion concentration ($5 \times 10^{-4}$ M) in the presence or absence of magnesium. However, changes in the CD spectrum upon binding of $Ca^{2+}$ and $Mg^{2+}$ ions to an undetermined number of relatively low affinity sites ($pK \leq 4$) have been observed in this laboratory by Dr. P. D. Chantler. Whether or not any of these sites is related to the high affinity $Ca^{2+}$ binding site present when the light chain is bound to myosin is not known.

The far UV CD spectra of the four molluscan regulatory light chains and the scallop SH-light chains were compared (Figure 5) and analyzed by the least-squares curve fitting procedure of Greenfield and Fasman (1969) to obtain rough estimates of the $\alpha$ helix, $\beta$ sheet, and so-called random structure. This analysis was carried out using their polylysine $\alpha$ helix, $\beta$ sheet, and random spectra and also with the spectrum of the scallop regulatory light chain in 6 M Gdn·HCl as a random basis spectrum. In general, use of the polylysine random basis spectrum resulted in very poor fits, indicating that it was probably not representative of the nonordered portions of the regulatory light chains. The Gdn·HCl random basis spectrum, on the other hand, gave much better fits. No alternative $\beta$ sheet or $\beta$ turn basis spectra were tried; therefore, it is not known whether the Gdn·HCl spectrum merely com-

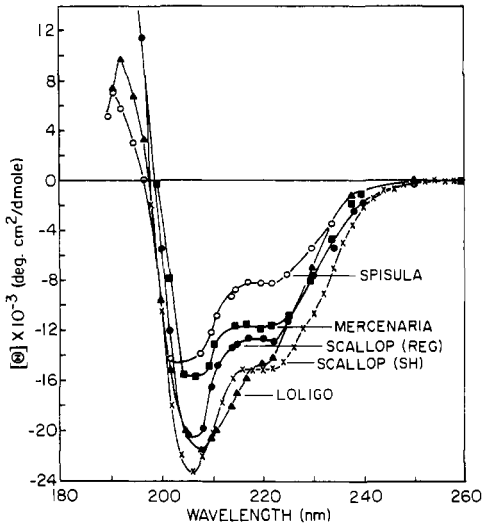


FIGURE 5: Comparative CD spectra of the various light chains in 0.1 M NaF, 0.01 M phosphate, pH 7.5.

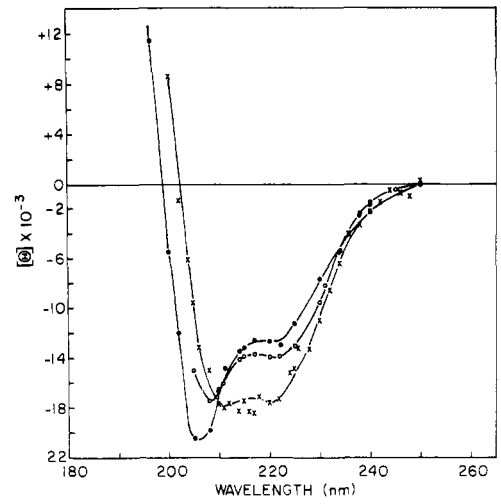


FIGURE 6: Variation of the CD spectrum of the scallop regulatory light chain as a function of pH. Filled circles (●), pH 12.2; open circles (○), pH 5.6; and crosses (X), pH 1.8.

pensated for a bad $\beta$ basis spectrum or whether the Gdn·HCl spectrum truly represents the non-ordered regions. The relative amounts of $\beta$ and random structure, therefore, could not be estimated with any confidence. However, it is felt that the estimate of $\alpha$-helix content in the scallop regulatory light chain using the Gdn·HCl random basis spectrum probably is fairly reliable since the $\alpha$-helix basis spectrum is very nearly orthogonal to the other two (Baker and Isenberg, 1976). The value for the scallop regulatory light chain obtained this way was 29%. The fit is shown in Figure 4a. All the other light chains seemed to contain about 20–40% $\alpha$ helix, but generally worse fits were obtained for them using either random basis spectrum.

The pH dependence of the CD spectrum of the scallop regulatory light chain was also investigated (Figure 6). No changes were observed in the alkaline pH range up to pH 12.2. Changes were observed, however, at acid pH. At pH 1.8 some changes in the ellipticity at 205 and 220 nm were observed suggesting an increase in the $\alpha$-helix content. Smaller changes were observed at pH 5.6 showing mainly a decrease in the ellipticity associated with the nonordered portions of the spectrum (207 nm) with a slight increase in the presumed $\alpha$-helical contribution (220 nm). This change seems to be associated with dimer formation observed between pH 7.0 and pH 5.5 and will be the subject of another paper.

The far-UV CD spectrum of the scallop SH-light chain (Figure 5) is similar to the regulatory light chains but suggests that it may have slightly greater amounts of ordered internal structure. The CD spectrum of the rabbit DTNB light chain has been published by Holt and Lowey (1973) and is similar to the spectra of the regulatory light chains in both the near and far ultraviolet regions.

## Discussion

A common feature of the myosin light chains which were studied is their apparent structural asymmetry. The combined evidence from hydrodynamic and fluorescence decay anisotropy measurements indicates that they probably exist in solution as compact structures rather than as swollen spheres or random coils and can be represented by ellipsoidal models having a longest dimension of about 100 Å. The scallop regulatory light chain, in particular, appears to be comprised of regions of very stable structure which are thermally stable, ionic strength independent, and invariant over the alkaline pH range studied.

One of the questions which arises is whether or not the conformation of the light chains is the same when bound to myosin as when they are free in solution. Although there is no direct evidence concerning the conformation of the light chains on myosin, the indirect evidence suggests that they probably do exist on myosin in asymmetric conformation. The overall stability of the tertiary structure in solution combined with the recent observation by Kendrick-Jones and Jakes (1977) that the scallop regulatory light chain is very resistent to trypsin digestion both when bound to myosin and when free in solution suggests that no gross unfolding occurs upon detachment of the light chain from myosin. Only one trypsin sensitive bond is exposed after detachment, while no bonds are cleaved while it is attached to myosin.

The location of the light chains on the heads of rabbit myosin has been the subject of several recent investigations (Bagshaw, 1977; Weeds and Pope, 1977). Based on observations during proteolytic digestion of myosin to form HMM and S1 fragments, it has been concluded that the DTNB light chain is located near the S1/S2 interface. The DTNB light chain in the presence of divalent cations is capable of inhibiting proteolysis in this region. The apparent length of the light chains suggests that they are capable of spanning large regions of and forming multiple attachments to the myosin heads. Interaction between the two regulatory light chains has been inferred from the negative cooperativity observed for detachment of the regulatory light chains from myosin at 0 °C (Szent-Györgyi et al., 1973). While 1 mole of regulatory light chain could be removed easily by EDTA treatment with concomitant loss of calcium sensitivity, the second mole of light chain resisted such treatment. This observation suggested a model in which the two regulatory light chains interact to destabilize their attachment to the myosin heads. A priori, the interaction could be either direct or allosteric. Direct interaction between the scallop regulatory light chains to form side-to-side dimers in solution has been observed (Stafford, in preparation); however, the questions of whether or not this interaction can occur on myosin and whether or not it plays a role in the regulatory process have not been answered.

In summary, there are two major inferences that can be drawn from this investigation. First, the light chains appear

to be asymmetric with a length of about 100 Å. Second, the asymmetric structure seems to be very stable and probably is characteristic of the light chains when they are attached to myosin.

Acknowledgment

We thank Enoch Small and Irvin Isenberg for giving us a copy of their manuscript prior to publication and for helpful discussions. We thank Walter Gratzer for helpful discussions. We also thank Serge Timasheff and Gerald Fasman for the use of their circular dichroism spectrometers. We acknowledge the Feldberg Computer Center of Brandeis University for providing computer time.

References

Ackers, G. K. (1967), *J. Biol. Chem. 242,* 3237.
Ackers, G. K. (1970), *Adv. Protein Chem. 24,* 343.
Ansevin, A. T., Roark, D. E., and Yphantis, D. A. (1970), *Anal. Biochem. 34,* 237.
Bagshaw, C. R. (1977), *Biochemistry 16,* 59.
Baker, C. C., and Isenberg, I. (1976), *Biochemistry 15,* 629.
Cassasa, E. F., and Eisenberg, H. (1964), *Adv. Protein Chem. 19,* 287.
Cohn, E. J., and Edsall, J. T. (1941), Proteins, Amino Acids and Peptides, New York, N.Y., Reinhold.
Dreizen, P., and Gershman, L. C. (1970), *Biochemistry 9,* 1688.
Dreizen, P., and Richards, D. H. (1973), *Cold Spring Harbor Symp. Quant. Biol. 37,* 29.
Dreizen, P., Gershman, L. C., Trotta, P. P., and Stracher, A. (1967), *J. Gen. Physiol. 50,* 85.
Ebashi, S. (1963), *Nature (London) 200,* 1010.
Ebashi, S., and Kodama, A. (1965), *J. Biochem. (Tokyo) 58,* 107.
Gautshi, W. (1965), in Handbook of Mathematical Functions, Abramowitz, M., and Stegan, I. A., Ed., New York, N.Y., Dover Publications, p 229.
Gazith, J. S., Himmelfarb, S., and Harrington, W. F. (1970), *J. Biol. Chem. 245,* 15.
Gershman, L. C., Dreizen, P., and Stracher, A. (1966), *Proc. Natl. Acad. Sci. U.S.A. 56,* 966.
Gershman, L. C., Stracher, A., and Dreizen, P. (1968), in Symposium on Fibrous Proteins, Australia, 1967, London, Butterworths.
Gershman, L. C., Stracher, A., and Dreizen, P. (1969), *J. Biol. Chem. 244,* 2726.
Greenfield, N., and Fasman, G. D. (1969), *Biochemistry 8,* 4108.
Harvey, S. C., and Cheung, H. C. (1977), *Biochemistry 16,* 5181.
Haschemeyer, R. H., and Haschemeyer, A. E. (1973), Proteins: A Guide to Study by Physical and Chemical Methods, New York, N.Y., Wiley.
Holt, J. C., and Lowey, S. (1975a), *Biochemistry 14,* 4600.
Holt, J. C., and Lowey, S. (1975b), *Biochemistry 14,* 4609.
Isenberg, I., Dyson, R. D., and Hanson, R. (1973), *Biophys. J. 13,* 1090.
Kendrick-Jones, J. (1974), *Nature (London) 249,* 631.
Kendrick-Jones, J., and Jakes, R. (1977), International Symposium Myocardial Failure, Munich, Tegernsee, June, 1976 (in press).
Kendrick-Jones, J., Lehman, W., and Szent-Györgyi, A. G. (1970), *J. Mol. Biol. 54,* 313.
Kendrick-Jones, J., Szentkiralyi, E. M., and Szent-Györgyi, A. G. (1972), *Cold Spring Harbor Symp. Quant. Biol. 37,* 47.
Kendrick-Jones, J., Szentkiralyi, E. M., and Szent-Györgyi, A. G. (1976), *J. Mol. Biol. 104,* 747.
Kuntz, I. D., and Kauzman, W. (1974), *Adv. Protein Chem. 28,* 239.
Lehman, W., Kendrick-Jones, J., and Szent-Györgyi, A. G. (1972), *Cold Spring Harbor Symp. Quant. Biol. 37,* 319.
Lehman, W., and Szent-Györgyi, A. G. (1975), *J. Gen. Physiol. 66,* 1.
Lowey, S., and Holt, J. C. (1973), *Cold Spring Harbor Symp. Quant. Biol. 37,* 19.
Pedersen, K. O. (1958), *J. Phys. Chem. 62,* 1282.
Roark, D. E., and Yphantis, D. A. (1969), *Ann. N.Y. Acad. Sci. 164,* 245.
Roark, D. E., and Yphantis, D. A. (1971), *Biochemistry 10,* 3241.
Sears, D. W., and Beychok, S. (1973), Circular Dichroism in Physical Principles and Techniques of Protein Chemistry, Leach, S. J., Ed., New York, N.Y., Academic Press.
Small, E. W., and Isenberg, I. (1977), *Biopolymers 16,* 1907.
Squire, P. G., and Li, C. H. (1961), *J. Am. Chem. Soc. 83,* 3521.
Stafford, W. F., III, and Szent-Györgyi, A. G. (1976), *Biophys. J. 16,* 70a.
Stafford, W. F., III, Szentkiralyi, E. M., and Szent-Györgyi, A. G. (1977), *Biophys. J. 17,* 120a.
Svedberg, T., and Pedersen, K. O. (1940), The Ultracentrifuge, London, Oxford University Press.
Szent-Györgyi, A. G. (1976), *Symp. Soc. Exp. Biol. 30,* 335.
Szent-Györgyi, A. G., Szentkiralyi, E. M., and Kendrick-Jones, J. (1973), *J. Mol. Biol. 74,* 179.
Szuchet, S., and Yphantis, D. A. (1973), *Biochemistry 12,* 5115.
Tanford, C. (1961), Physical Chemistry of Macromolecules, New York, N.Y., Wiley.
Tsao, T. C. (1953), *Biochim. Biophys. Acta 11,* 368.
Wagner, P. D., and Weeds, A. G. (1977), *J. Mol. Biol. 109,* 455.
Weeds, A. G. (1969), *Nature (London) 223,* 1362.
Weeds, A. G., and Pope, B. (1977), *J. Mol. Biol. 111,* 129.
Winstanley, M. A., Trayer, H. R., and Trayer, I. P. (1977), *FEBS Lett. 77,* 239.
Yguerabide, J. (1972), *Methods Enzymol. 266,* 498.
Yphantis, D. A. (1964), *Biochemistry 3,* 297.